

FREQUENCY SPECTRUM OF ELASTIC WAVES
IN BODY CENTERED CUBIC LATTICES

by

BUNNY COWAN CLARK

B.S., Kansas State University, 1958

A THESIS

submitted in partial fulfillment of the

requirements for the degree

MASTER OF SCIENCE

Department of Physics

KANSAS STATE UNIVERSITY

Approved:

1963



LD
2668
T4
1/10/53
E-7
C.2
Document

TABLE OF CONTENTS

INTRODUCTION.	1
DERIVATION OF LATTICE EQUATIONS OF MOTION	4
SOLUTION OF THE EQUATIONS OF MOTION	13
RELATIONSHIPS BETWEEN ELASTIC CONSTANTS AND LATTICE FORCE CONSTANTS	18
CALCULATION OF THE FREQUENCY DISTRIBUTION	24
RESULTS	26
CONCLUSIONS	42
ACKNOWLEDGMENTS	44
REFERENCES	45

INTRODUCTION

The dynamics of crystal lattices have been of interest for some time, especially with regard to the vibrational motion of the lattice points. In 1912 Debye (1) obtained a frequency distribution by treating the solid as a continuum. At that time the specific heat obtained from the Debye frequency distribution agreed well with experiment; however, the theory was in disagreement with the known periodic structure of crystals. Born and von Karman (2) in 1912 examined the dynamics of a lattice of discrete particles, however their method was computationally more complicated than the Debye theory and the simpler theory continued in use until its inability to fit experimental data at low temperatures became apparent. Blackman in 1935 (3) and 1937 (4) revived the Born-von-Karman treatment, and his work indicated that the Born-von-Karman frequency distribution had the characteristics necessary for better agreement with experiment. Blackman's calculations for a two dimensional lattice were later shown to be correct by exact calculations of Montroll (5) and Bowers and Rosenstock (6). The revival of interest in the Born-von-Karman method has stimulated theoretical investigations on the general characteristics of the frequency distribution by such workers as Van Hove (7) and Phillips (8) among others.

With the return of the non-continuum treatment of crystal lattices the question of the types of interactions between lattice points became pertinent. Perhaps the most common method for cubic crystals assumes central forces between nearest and next nearest neighbors. This central force model was used by Blackman in his calculations for two dimensional lattices. It has also been used by Bowers and Rosenstock (6), and by Montroll (5) in

obtaining exact frequency distributions for two dimensional lattices. The central force model was used by Fine (9) and later Clark (10) in obtaining frequency distributions for body centered cubic crystals, and by Leighton (11) for face centered cubic crystals. Recently Shankland (12) has used the central force model for both face centered and body centered cubic crystals. Montroll and Peasly (13) used central forces in calculating the frequency distribution of body centered cubic crystals using Montroll's (14) moment method.

Although it has been customary to assume a central force model, this assumption leads to the Cauchy relationship between the elastic constants of the crystal, a relationship which is not born out by experiment. Owing to the prediction of the Cauchy relationship from the use of central forces alone various models incorporating non-central forces have been examined. Smith (15) proposed a model for the diamond lattice including arbitrary forces between nearest neighbors, and central forces between next-nearest neighbors. Rosenstock and Newell (16) have examined a simple cubic lattice using non-central forces between nearest neighbors, and Singh and Bowers (17) have examined a body centered cubic crystal using non-central forces between nearest neighbors and central forces between next-nearest neighbors. This paper treats a body centered cubic lattice using non-central forces of the type introduced by Gazis, Herman, and Wallis (18) in treating surface waves in a simple cubic crystal. In this model non-central forces consisting of angular stiffness forces associated with primitive angles of the lattice are included along with the central forces between nearest and next-nearest neighbors. The addition of this third force constant makes it possible to derive explicit relationships between the elastic constants of the crystal and the lattice

model force constants. In addition to the angles considered by Gazis et. al., additional angles, formed with one side the nearest neighbor distance and the other side the next-nearest neighbor distance, were included in this work. The addition of the second angular terms resulted in four force constants which were matched with the three elastic constants by assuming a relationship between the two angular force constants.

As is usual plane wave solutions to the equations of motion are assumed resulting in a secular equation in the square of the frequency. The roots of this equation were found at approximately 39,000 solution points within the first $1/48$ th Brillouin zone using an IBM 7090 digital computer. Frequency distribution histograms were constructed by determining the number of modes of oscillation within specified frequency intervals. When the non-central forces are ignored this model reduces to the ordinary central force model, and in this case the calculations agree with the previous work of Fine (9) and Clark (10).

One of the primary aims of the investigation was to examine the effect of the inclusion of non-central forces on the frequency distribution. Comparison between the central force model and the model employed here was made for tungsten which is essentially isotropic and vanadium which is one of the more anisotropic body centered cubic crystals. The calculations with vanadium were also compared with the frequency distributions obtained by the slow neutron experiments of Steward and Brockhous (19), and Eisenhauer et. al. (20). Dispersion curves along specified directions were calculated in order to compare the model with the experimentally determined dispersion curves of Low (21) for iron.

DERIVATION OF LATTICE EQUATIONS OF MOTION

The equations of motion for the Born-von-Karman model of the crystal lattice are required to compute the vibrational modes of a crystal. The nature of the interactions between the lattice points must be assumed. Perhaps the most common assumption is the approximation that the only interactions are central forces between nearest and next-nearest neighbors of the crystal lattice. The model used here for a body centered cubic lattice of identical particles assumes non-central angular stiffness forces between primitive and secondary angles of the lattice as well as the usual central forces between nearest and next-nearest neighbors.

Figure 1 shows the configuration of the lattice points and the indexing of these points. A vector \bar{S}_j will refer to a general infinitesimal displacement of the j th atom in the lattice. The displacement vector \bar{S}_j has components (u_j, v_j, w_j) in the $x, y,$ and z directions. Although the equations of motion for central forces appear elsewhere, for example in DeLaunay (22), they will be repeated here in order to provide a continuity of notation.

The central force between nearest neighbors may be represented by

$$\bar{F}_{nn} = \alpha \sum_{nn} \bar{\epsilon}_j [\bar{\epsilon}_j \cdot (\bar{S}_j - \bar{S}_0)] , \quad (1)$$

where α is the nearest neighbor force constant and $\bar{\epsilon}_j$ is a unit vector with components $\frac{1}{\sqrt{3}} (\mu_j, \nu_j, \eta_j)$ with direction along the line of action between the central atom and the n th atom and the sum is over all nearest neighbors (nn). The components μ_n, ν_n, η_n take on the values ± 1 depending on the location of the n th atom. Expanding the scalar product in Eq. (1), we may write the force acting on the central atom in the x -direction as follows:

EXPLANATION OF PLATE I

Fig. 1. The indexing of a body centered cubic lattice using $1/2$ the lattice spacing as the basic unit.

EXPLANATION OF PLATE II

- Fig. 2. Body centered cubic lattice showing primitive (θ_1) and secondary (θ_2) angles.
- Fig. 3. Illustration of the two triangles considered in deriving the angular stiffness forces.

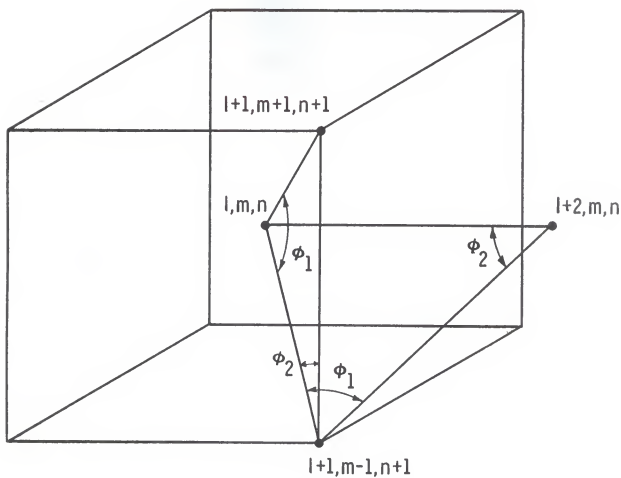


Figure 2

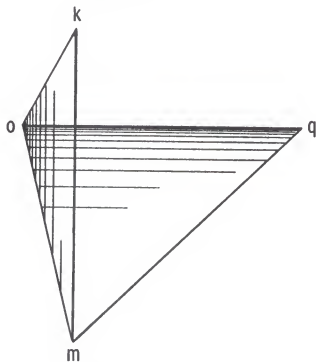


Figure 3

72 secondary angles of the type ϕ_2 in Fig. 2 having a force constant γ_2 . To find the potential function given by Eq. (5) it is necessary first to construct the vectors \bar{n} . In order to construct these vectors only the indexing of the two identical triangles shown in Fig. 3 need be examined. In this figure the point labeled o refers to the center atom, m and k to atoms on the cube corners, and q to a next-nearest neighbor atom. The vectors \bar{x}_k , \bar{x}_m , and \bar{x}_q , each drawn from the origin to the atom under consideration, are conveniently found by taking their components to be the differences of the indices of the kth, mth, or qth atom from those of the center atom, namely ℓ , m, n. For example, if the kth atom is the $\ell+1$, $m+1$, $n+1$ lattice point then \bar{x}_k has all components equal to one. The vectors \bar{n} may now be taken as a linear combination of the vectors \bar{x}_k and \bar{x}_m in triangle kom which will be called a type 1 triangle, and $-\bar{x}_m$ and $(\bar{x}_m - \bar{x}_q)$ in triangle omz which is designated type 2. There is the added condition that the vectors \bar{n} be normal to the sides of the angles and in the direction of decreasing angle. It should be mentioned that the choice of the direction of the \bar{n} is arbitrary but must be consistent. The derivation of the non-central force on the center atom will be carried out for triangles of type 1, only, as a simple transformation will give the contribution due to triangles including a next-nearest neighbor atom. The force on the central atom due to angular deformations of the first type triangle may be written as

$$\begin{aligned}
 \bar{F}_1 &= -\frac{1}{2} \nabla_o V_1 \\
 &= -\frac{1}{2} \sum_{\text{Type 1}} \{ \nabla_o [\gamma_1 (C_1 (\bar{s}_k - \bar{s}_o) \cdot \bar{n}_{ko} + C_1 (\bar{s}_m - \bar{s}_o) \cdot \bar{n}_{mo})^2 \\
 &\quad + \gamma_2 (C_2 (\bar{s}_k - \bar{s}_m) \cdot \bar{n}_{km} + C_1 (\bar{s}_o - \bar{s}_m) \cdot \bar{n}_{mo})^2 \\
 &\quad + \gamma_2 (C_2 (\bar{s}_m - \bar{s}_k) \cdot \bar{n}_{km} + C_1 (\bar{s}_o - \bar{s}_k) \cdot \bar{n}_{ko})^2] \}
 \end{aligned} \tag{6}$$

where

$$\nabla_0 = \bar{i} \frac{\partial}{\partial u_0} + \bar{j} \frac{\partial}{\partial v_0} + \bar{k} \frac{\partial}{\partial w_0} .$$

In this equation C_1 and C_2 are constants which take into account the difference in the lengths of the sides of the angles and the magnitudes of the normal vectors.

The normal vectors \bar{n}_{ko} , \bar{n}_{mo} , and \bar{n}_{km} are defined by the equations

$$\begin{aligned} \bar{n}_{ko} &= \bar{x}_m - e \bar{x}_k \\ \bar{n}_{mo} &= \bar{x}_k - e \bar{x}_m \\ \bar{n}_{km} &= -(\bar{x}_k + \bar{x}_m) \end{aligned} \quad (7)$$

where

$$e = \frac{\bar{x}_k \cdot \bar{x}_m}{\bar{x}_k \cdot \bar{x}_k} = \cos \vartheta . \quad (8)$$

The change in potential energy, V_2 , due to angular changes in type 2 triangles may be written directly from the potential function V_1 in Eq. (6) as the triangles are identical except for labeling. Referring to Fig. 3, the potential function V_2 is obtained from V_1 by the following transformations of indices

$$\begin{aligned} m &\rightarrow p , \\ k &\rightarrow q , \\ p &\rightarrow n , \end{aligned}$$

and by letting

$$\begin{aligned} \bar{x}_m &\rightarrow -\bar{x}_m , \\ \bar{x}_k &\rightarrow (\bar{x}_q - \bar{x}_m) . \end{aligned} \quad (9)$$

The expansions of Eqs. (6) and the resulting expression with the substitutions given in (9) give the angular forces in the x-direction in terms of displacements of the lattice points in the x, y, and z directions. The expansions are quite tedious but straightforward. The total contribution from the angular term results in a force on the central atom, in the x direction, given by:

$$\begin{aligned} \bar{i} \cdot \bar{F}_A = \gamma_1 C_1^2 \{ & u_{\ell, m, n} [-32(1-e)^2 - 8(3-2e+3e^2) + 8(1-e)^2 U - 8e(1-e)(V+W) \\ & + 4(1+e)^2 (u_{\ell+2, m, n} + u_{\ell-2, m, n}) - 4(1-e)^2 (u_{\ell, m+2, n} + u_{\ell, m-2, n} + u_{\ell, m, n+2} + u_{\ell, m, n-2})] \} \\ & + \gamma_2 \{ 8u_{\ell, m, n} [-20C_1^2(3-2e+3e^2) + 8C_1 C_2(1-e) - 16C_2^2] \\ & + U[20C_1^2(3-2e+3e^2) + (V+W)[20C_1^2(3e^2-2e-1) + 8C_1 C_2(1+e)] \\ & + [32C_2^2 - 16C_1 C_2(1-e)] (u_{\ell, m+2, n} + u_{\ell, m-2, n} + u_{\ell, m, n+2} + u_{\ell, m, n-2}) \} \end{aligned} \quad (10)$$

where

$$\begin{aligned} U = & (u_{\ell+1, m+1, n+1} + u_{\ell+1, m+1, n-1} + u_{\ell+1, m-1, n+1} + u_{\ell+1, m-1, n-1} \\ & + u_{\ell-1, m+1, n+1} + u_{\ell-1, m+1, n-1} + u_{\ell-1, m-1, n+1} + u_{\ell-1, m-1, n-1}) \\ V = & (v_{\ell+1, m+1, n+1} + v_{\ell+1, m+1, n-1} - v_{\ell+1, m-1, n+1} - v_{\ell+1, m-1, n-1} \\ & + v_{\ell-1, m+1, n+1} - v_{\ell-1, m+1, n-1} + v_{\ell-1, m-1, n+1} + v_{\ell-1, m-1, n-1}) \\ W = & (w_{\ell+1, m+1, n+1} - w_{\ell+1, m+1, n-1} + w_{\ell+1, m-1, n+1} - w_{\ell+1, m-1, n-1} \\ & + w_{\ell-1, m+1, n+1} + w_{\ell-1, m+1, n-1} - w_{\ell-1, m-1, n+1} + w_{\ell-1, m-1, n-1}) \end{aligned} \quad (11)$$

For small relative displacements the motion of the other lattice points may be related to the displacement of the central atom and its spatial derivatives by a Taylor series expansion about the central atom. In the limit of small displacements, however, the coefficient of the first order term $u_{\ell, m, n}$ must tend to zero. This condition is satisfied by Eq. (10) when e is replaced by its value, $1/3$, as found from Eq. (6). It is also desirable that

the non-central forces discussed here be invariant under rigid body rotations. Equation (10) satisfies this condition for the ratio $C_1/C_2 = 1/2$, which takes into account the difference in the lengths of the sides of the angles and the different magnitudes of the normal vectors.

The equation for the force in the x-direction on the central atom due to the central and non-central forces considered here may now be written as

$$\begin{aligned}
 F_x &= m \ddot{u}_{\ell, m, n} \\
 &= -u_{\ell, m, n} \left[\frac{8}{3} \alpha + 2\beta + 20 \gamma_1 \left(\frac{16}{9} \right) + 30 \gamma_2 \left(\frac{16}{9} \right) \right] \\
 &\quad + [\beta + 4\gamma_1 \left(\frac{16}{9} \right)] [u_{\ell+2, m, n} + u_{\ell-2, m, n}] + [-\gamma_1 \left(\frac{16}{9} \right) + \frac{3}{2} \gamma_2 \left(\frac{16}{9} \right)] \\
 &\quad (u_{\ell, m+2, n} + u_{\ell, m-2, n} + u_{\ell, m, n+2} + u_{\ell, m, n-2}) \\
 &\quad + U \left[\frac{\alpha}{3} + 2 \gamma_1 \left(\frac{16}{9} \right) + 3 \gamma_2 \left(\frac{16}{9} \right) \right] + (V+W) \left[\frac{\alpha}{3} - \gamma_1 \left(\frac{16}{9} \right) + \frac{3}{2} \gamma_2 \left(\frac{16}{9} \right) \right], \tag{12}
 \end{aligned}$$

where U, V, and W are defined as in Eq. (11). The forces in the y and z directions on the central atom are found by a circular permutation of u, v, and w.

SOLUTION OF THE EQUATIONS OF MOTION

The solutions of the equations of motion are assumed to be plane waves, where the usual cyclic boundary conditions of Born (23) are applied; they insure the presence of the characteristic frequencies of the crystal. As the body centered cubic lattice is a Bravais lattice, the position vector \bar{r} of any atom in the lattice may be expressed as a linear combination with integer coefficients of three basis vectors $\bar{a}_1, \bar{a}_2, \bar{a}_3$. This results in a considerable reduction in the number of plane wave solutions which must be included, for, if the motion of the center atom is given by

$$\begin{aligned}u_o &= U \exp 2\pi i (vt + \bar{k} \cdot \bar{r}_o) \\v_o &= V \exp 2\pi i (vt + \bar{k} \cdot \bar{r}_o) \\w_o &= W \exp 2\pi i (vt + \bar{k} \cdot \bar{r}_o),\end{aligned}$$

then the motion of any other atom, say the n th, may be written as

$$\begin{aligned}u_n &= U \exp 2\pi i (vt + \bar{k} \cdot \bar{r}_n) \\v_n &= V \exp 2\pi i (vt + \bar{k} \cdot \bar{r}_n) \\w_n &= W \exp 2\pi i (vt + \bar{k} \cdot \bar{r}_n).\end{aligned}$$

Here $U, V,$ and W are the components of the plane wave amplitude, and \bar{k} is a propagation vector in the reciprocal lattice whose magnitude is the reciprocal of the wave length. The values of \bar{k} are restricted to the first Brillouin zone, as discussed by Brillouin (24). A convenient set of basis vectors $\bar{a}_1, \bar{a}_2,$ and \bar{a}_3 is shown in Fig. 4. Using these vectors one may write \bar{r} as

$$\bar{r} = n_1 \bar{a}_1 + n_2 \bar{a}_2 + n_3 \bar{a}_3$$

EXPLANATION OF PLATE III

Fig. 4. A set of basis vectors for a body centered cubic lattice.

PLATE III

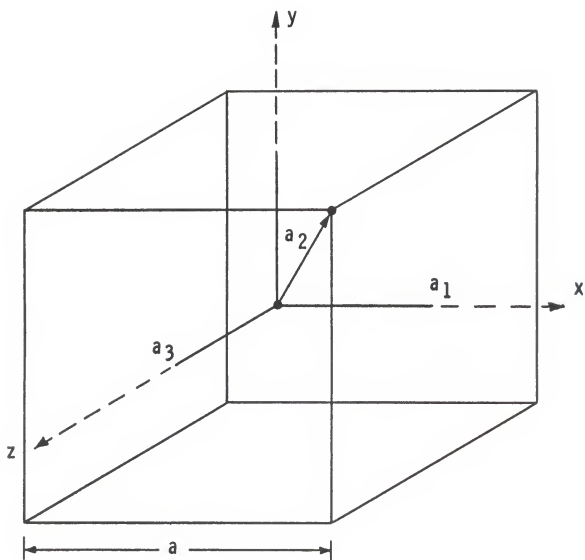


Figure 4

where n_1 , n_2 , and n_3 are integers.

If, however, \bar{e}_1 , \bar{e}_2 , and \bar{e}_3 are unit vectors parallel to the x, y, and z coordinate axis and a is the cube edge length, then the vector \bar{r} may be written in the form used by De Launay (22), namely,

$$\bar{r} = (n_1 + \frac{n_2}{2}) a \bar{e}_1 + \frac{n_2}{2} a \bar{e}_2 + (n_3 + \frac{n_2}{2}) \bar{e}_3. \quad (13)$$

The vector \bar{k} may also be written with components k_1 , k_2 , and k_3 parallel to the x, y, z coordinate axis. The substitution of these solutions into the equations of motion gives three homogeneous linear equations in U, V, and W. A non-trivial solution requires that the determinant of the coefficients of U, V, and W vanish, which determines the possible values of the frequency.

This secular determinant is

$$\begin{vmatrix} A_1 + m\omega^2 & B & C \\ B & A_2 + m\omega^2 & D \\ C & D & A_3 + m\omega^2 \end{vmatrix} = 0, \quad (14)$$

where

$$\begin{aligned} A_1 = & - \left[8 \frac{\alpha}{3} + 16 \gamma_1 \left(\frac{16}{9} \right) + 24 \gamma_2 \left(\frac{16}{9} \right) \right] (1 - \cos \phi_1 \cos \phi_2 \cos \phi_3) \\ & - 4\beta \sin^2 \phi_1 + 2 \gamma_1 \left(\frac{16}{9} \right) (5 \cos 2 \phi_1 - \cos 2 \phi_2 - \cos 2 \phi_3) \\ & - 3 \gamma_2 \left(\frac{16}{9} \right) (2 + \cos 2 \phi_1 - \cos 2 \phi_2 - \cos 2 \phi_3) \end{aligned} \quad (15)$$

$$B = - 8 \left[\frac{\alpha}{3} - \gamma_1 \left(\frac{16}{9} \right) + \gamma_2 \left(\frac{16}{9} \right) \left(\frac{3}{2} \right) \right] \cos \phi_3 \sin \phi_1 \sin \phi_2$$

$$C = - 8 \left[\frac{\alpha}{3} - \gamma_1 \left(\frac{16}{9} \right) + \gamma_2 \left(\frac{16}{9} \right) \left(\frac{3}{2} \right) \right] \cos \phi_2 \sin \phi_1 \sin \phi_3$$

$$D = - 8 \left[\frac{\alpha}{3} - \gamma_1 \left(\frac{16}{9} \right) + \gamma_2 \left(\frac{16}{9} \right) \left(\frac{3}{2} \right) \right] \cos \phi_1 \sin \phi_2 \sin \phi_3$$

In Eq. (15) the quantity $\phi_i = \pi a k_i$, $i = 1, 2, 3$, is used for convenience.

The quantity a is the distance between next-nearest neighbors for the body

EXPLANATION OF PLATE IV

Fig. 5. The first Brillouin zone for a body centered cubic lattice with the $1/48$ th zone accentuated.

PLATE IV

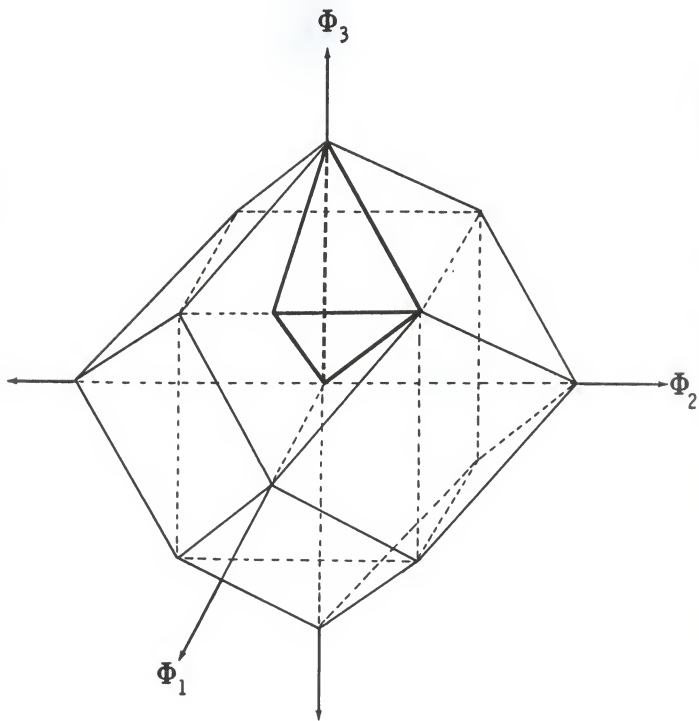


Figure 5

RELATIONSHIPS BETWEEN ELASTIC CONSTANTS AND LATTICE FORCE CONSTANTS

In the limit of long wavelengths where the wavelength is much greater than the lattice spacing the plane waves are effectively propagating in a continuous medium. This allows the identification of the lattice force constants with the elastic constants of the medium found from measurements of the velocity of sound. The problem then becomes the formulation of the equations of motion governing small displacements in an homogeneous medium. This problem in classical mechanics is discussed in many texts on the subject, for example, the necessary equations are presented by Joos (26),

Theoretical Physics, Chapter VIII. The relationship between strains and stresses is given by Hooke's Law

$$P_{ij} = \sum_{\ell} \sum_m T_{ij\ell m} \epsilon_{\ell m} \quad , \quad i, j, \ell, m = 1, 2, 3, \quad (17)$$

where P_{ij} is the stress tensor, $\epsilon_{\ell, m}$ is the strain tensor, and $T_{ij\ell m}$ is a tensor of fourth rank. As is customary, the six independent components of the strain tensor will be represented by e_{ij} where

$$e_{ii} = \epsilon_{ii} \quad , \quad e_{ij} = 2\epsilon_{ij} \quad \quad i \neq j$$

Then from Joos (26), p. 166, the e_{ij} are defined by

$$e_{11} = \frac{\partial u}{\partial x} \quad , \quad e_{22} = \frac{\partial v}{\partial y} \quad , \quad e_{33} = \frac{\partial w}{\partial z} \quad ,$$

$$e_{23} = \frac{\partial v}{\partial z} + \frac{\partial w}{\partial y} \quad , \quad e_{13} = \frac{\partial w}{\partial x} + \frac{\partial u}{\partial z} \quad , \quad e_{12} = \frac{\partial u}{\partial y} + \frac{\partial v}{\partial x} \quad ,$$

where u , v , and w are the rectangular components of the displacement. The elements of T may be identified with the elastic constants of the medium in Voigt's notation. In this notation the linear relationship between stress

and strain may be written in matrix notation as

$$\bar{P} = C\bar{e}$$

where \bar{P} is a row vector whose elements are the six independent elements of the stress tensor, and \bar{e} is a row vector with the six independent elements of the strain tensor as components. The matrix C in general has 21 independent elements C_{rs} which are related to the tensor elements T_{ijkl} . For materials with cubic symmetry, as shown by Zener (27), C reduces to the matrix

$$C = \begin{vmatrix} C_{11} & C_{12} & C_{12} & 0 & 0 & 0 \\ C_{12} & C_{11} & C_{12} & 0 & 0 & 0 \\ C_{12} & C_{12} & C_{11} & 0 & 0 & 0 \\ 0 & 0 & 0 & C_{44} & 0 & 0 \\ 0 & 0 & 0 & 0 & C_{44} & 0 \\ 0 & 0 & 0 & 0 & 0 & C_{44} \end{vmatrix} \quad (18)$$

With the aid of Eq. (18) the relationships between the stresses and the displacements may be found.

The equations of motion for the continuum are obtained from the elastic equilibrium between the body forces and the stresses, which, as given by Joos (26), p. 174, are

$$\begin{aligned} g_x + \frac{\partial P_{11}}{\partial x} + \frac{\partial P_{12}}{\partial y} + \frac{\partial P_{13}}{\partial z} &= 0, \\ g_y + \frac{\partial P_{12}}{\partial x} + \frac{\partial P_{22}}{\partial y} + \frac{\partial P_{23}}{\partial z} &= 0, \\ g_z + \frac{\partial P_{13}}{\partial x} + \frac{\partial P_{23}}{\partial y} + \frac{\partial P_{33}}{\partial z} &= 0, \end{aligned} \quad (19)$$

where g_x , g_y , and g_z are the components of the body forces acting on a unit

volume. In the absence of external body forces $g_x = -\rho \frac{\partial^2 u}{\partial t^2}$, the inertial force per unit volume, and upon substitution for P_{ij} in terms of e_{ij} , Eq. (19) becomes the wave equation

$$\begin{aligned} \rho \frac{\partial^2 u}{\partial t^2} = & (C_{11} - C_{12}) \frac{\partial^2 u}{\partial x^2} + C_{12} \left(\frac{\partial^2 u}{\partial x^2} + \frac{\partial^2 v}{\partial x \partial y} + \frac{\partial^2 w}{\partial x \partial y} \right) \\ & + C_{44} \left(\frac{\partial^2 u}{\partial y^2} + \frac{\partial^2 u}{\partial z^2} + \frac{\partial^2 v}{\partial x \partial y} + \frac{\partial^2 w}{\partial x \partial z} \right), \end{aligned} \quad (20)$$

with similar equations in the y and z directions. Assuming plane wave solutions of the form

$$u = U \exp 2\pi i (vt + \bar{k} \cdot \bar{r})$$

$$v = V \exp 2\pi i (vt + \bar{k} \cdot \bar{r})$$

$$w = W \exp 2\pi i (vt + \bar{k} \cdot \bar{r})$$

results in the secular determinant

$$\begin{vmatrix} (C_{11} - C_{44}) k_1^2 + C_{44} k^2 - \rho v^2 & (C_{12} + C_{44}) k_1 k_2 & (C_{12} + C_{44}) k_1 k_3 \\ (C_{12} + C_{44}) k_1 k_2 & (C_{11} - C_{44}) k_2^2 + C_{44} k^2 - \rho v^2 & (C_{12} + C_{44}) k_2 k_3 \\ (C_{12} + C_{44}) k_1 k_3 & (C_{12} + C_{44}) k_1 k_3 & (C_{11} - C_{44}) k_3^2 + C_{44} k^2 - \rho v^2 \end{vmatrix} = 0 \quad (21)$$

restricting the values of the frequency. A review of this material is given by De Launay (22), p. 265.

The identification of the lattice force constants may now be made either from Eq. (20) or Eq. (21). In both cases the limiting condition of small relative displacements, i.e. wavelengths long compared to the lattice spacing, is made. If, in Eq. (12) representing the motion of the center atom in the x-direction, we expand the displacements to second order about the central

atom a comparison with Eq. (20) may be made. In Eq. (20), for a body centered cubic lattice, $\rho = 2m/a^3$, where a is the lattice spacing. An equally convenient comparison may be made in the limiting case of long wavelengths from the secular Eq. (14) by replacing $\sin \phi_1$ by ϕ_1 and $\cos \phi_1$ by $1 - \phi_1^2/2$. In either case the following relationships hold:

$$\begin{aligned} a C_{11} &= 2 \left(\frac{\alpha}{3} + \beta + 6 \gamma_1' + 3 \gamma_2' \right) \\ a C_{12} &= 2 \left(\frac{\alpha}{3} - 3 \gamma_1' + \frac{9}{2} \gamma_2' \right) \\ a C_{44} &= 2 \left(\frac{\alpha}{3} + \gamma_1' + \frac{3}{2} \gamma_2' \right) \end{aligned} \quad (22)$$

where

$$\gamma_1' = \left(\frac{16}{9} \right) \gamma_1 \quad \text{and} \quad \gamma_2' = \left(\frac{16}{9} \right) \gamma_2$$

If $\gamma_2 = 0$, for example, the above three equations determine the lattice force constants uniquely, otherwise the lattice parameters are determined only within a given ratio of γ_2/γ_1 . Figure 6 shows the variation of β/α with ratios of γ_2/γ_1 for the element vanadium. The elastic constants for vanadium are those of Alers (28). Solving Eqs. (22) for α , β , γ , in order to show the dependence of the lattice force constants, one obtains:

$$\begin{aligned} \alpha &= \frac{3}{8} a (C_{12} + 3 C_{44}) - 9 \gamma_2' \\ \beta &= C_{11} \frac{a}{2} + \frac{5}{8} C_{12} a - \frac{9}{8} C_{44} a + 9 \gamma_2' \\ \gamma_1' &= \frac{a}{8} (C_{44} - C_{12}) - \frac{6}{4} \gamma_2' \end{aligned} \quad (23)$$

Thus if γ_2 is zero, γ_1 is negative for all elements in which C_{44} is

less than C_{12} . There are, however, experimental elastic constants such as those for sodium given by Quimby and Siegel (25) at 150°K where C_{44} is greater than C_{12} in which case γ_1 is positive with γ_2 equal to zero.

EXPLANATION OF PLATE V

Fig. 6. The variation of β/α with γ_1/γ_2 for the element vanadium.

PLATE V

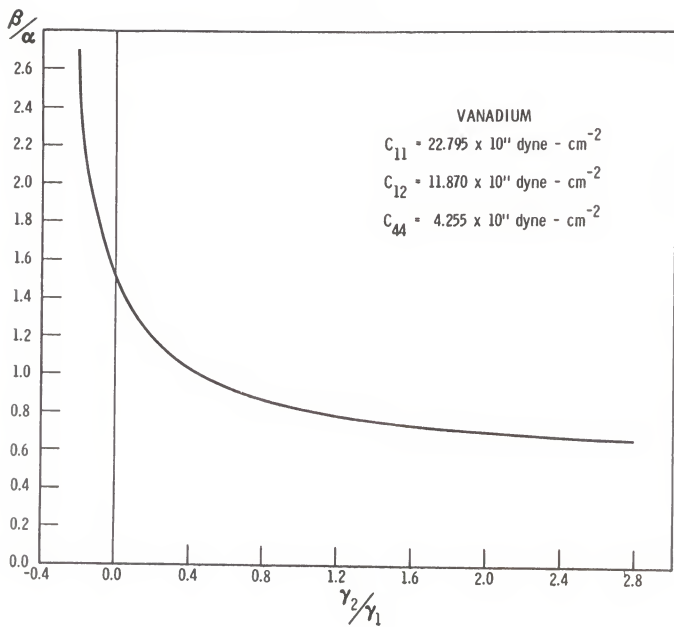


Figure 6

with the experimental maximum frequency. Table 3 gives the frequency histograms for vanadium for ratios of γ_2/γ_1 of 0.5 and 1.0, and Fig. 7 shows the frequency histograms for these ratios along with the case for $\gamma_2 = 0$. Figure 7 indicates that increasing the ratio of γ_2/γ_1 reduces the power of the first peak and moves the two maxima closer together producing better agreement with experiment. It was not the object of this paper to initiate a parameter study; however, it does seem that the availability of the additional force constant γ_2 may be used to alter the shapes of the calculated frequency distribution in order to obtain better agreement with experiment.

To better understand the effect that the elastic constants play in the determination of the frequency distribution vanadium distributions were calculated using $\pm 10\%$ values for each elastic constant independently and with $\gamma_2 = 0$. The resulting frequency histograms are given in Table 4, and, briefly, it is noted that increasing C_{12} or C_{11} by 10% tends to spread the peaks while increasing C_{44} brings the maxima together slightly. It is also apparent that increasing C_{11} and C_{44} by 10% increases the sharpness of the low frequency peak while increasing C_{12} has the opposite effect. None of these frequency distributions seem to fit experiment appreciably better than the distribution with the unchanged elastic constants, and as shown in Table 5, the calculated maximum frequencies are all in the neighborhood of the experimental maximum. Clark (10) has calculated the frequency distribution for vanadium and the model used here represents the experimental frequency distribution as well as the ordinary central force model used by Clark and predicts a maximum frequency in better agreement with experiment.

In addition to the frequency spectra discussed above the model was used to calculate frequency dispersion curves. The calculations were compared with

Table 3. Frequency histograms for vanadium with $\gamma_2/\gamma_1 = 0.5$ and 1.0.

Frequency interval	Fraction in interval $\gamma_2/\gamma_1 = 0.5$	Fraction in interval $\gamma_2/\gamma_1 = 1.0$	Frequency interval	Fraction in interval $\gamma_2/\gamma_1 = 0.5$	Fraction in interval $\gamma_2/\gamma_1 = 1.0$
0. - 0.01	0.	0.	0.50 - 0.51	0.02641256	0.02621722
0.01 - 0.02	0.	0.	0.51 - 0.52	0.02441675	0.02445073
0.02 - 0.03	0.00000849	0.00000849	0.52 - 0.53	0.02242944	0.02251437
0.03 - 0.04	0.00001698	0.00001698	0.53 - 0.54	0.02130839	0.02129141
0.04 - 0.05	0.00005945	0.00005945	0.54 - 0.55	0.02013639	0.01996654
0.05 - 0.06	0.00007643	0.00007643	0.55 - 0.56	0.01939752	0.01918520
0.06 - 0.07	0.00011040	0.00011040	0.56 - 0.57	0.01841235	0.01830195
0.07 - 0.08	0.00016136	0.00016136	0.57 - 0.58	0.01769046	0.01765650
0.08 - 0.09	0.00024629	0.00024629	0.58 - 0.59	0.01702803	0.01690064
0.09 - 0.10	0.00029724	0.00029724	0.59 - 0.60	0.01616177	0.01631464
0.10 - 0.11	0.00037368	0.00038217	0.60 - 0.61	0.01485388	0.01573713
0.11 - 0.12	0.00045861	0.00045011	0.61 - 0.62	0.01294300	0.01526153
0.12 - 0.13	0.00056052	0.00055203	0.62 - 0.63	0.01174552	0.01464156
0.13 - 0.14	0.00066243	0.00067092	0.63 - 0.64	0.01109158	0.01421692
0.14 - 0.15	0.00078983	0.00078133	0.64 - 0.65	0.01039517	0.01319779
0.15 - 0.16	0.00096817	0.00096817	0.65 - 0.66	0.00993656	0.01195784
0.16 - 0.17	0.00101913	0.00098516	0.66 - 0.67	0.00950342	0.01044612
0.17 - 0.18	0.00120597	0.00123994	0.67 - 0.68	0.00907029	0.00968177
0.18 - 0.19	0.00140131	0.00132487	0.68 - 0.69	0.00875606	0.00909577
0.19 - 0.20	0.00152870	0.00156267	0.69 - 0.70	0.00851826	0.00880702
0.20 - 0.21	0.00177499	0.00173253	0.70 - 0.71	0.00833991	0.00831443
0.21 - 0.22	0.00197881	0.00197881	0.71 - 0.72	0.00820403	0.00836539
0.22 - 0.23	0.00223360	0.00219113	0.72 - 0.73	0.00807664	0.00780486
0.23 - 0.24	0.00244592	0.00237798	0.73 - 0.74	0.00801718	0.00800020
0.24 - 0.25	0.00261577	0.00267522	0.74 - 0.75	0.00799171	0.00764351
0.25 - 0.26	0.00308288	0.00298096	0.75 - 0.76	0.00821252	0.00781336
0.26 - 0.27	0.00319328	0.00318479	0.76 - 0.77	0.00833142	0.00788979
0.27 - 0.28	0.00365189	0.00350752	0.77 - 0.78	0.00869661	0.00806814
0.28 - 0.29	0.00400859	0.00388120	0.78 - 0.79	0.00903632	0.00818704
0.29 - 0.30	0.00439077	0.00428885	0.79 - 0.80	0.00999600	0.00868811
0.30 - 0.31	0.00471349	0.00466254	0.80 - 0.81	0.01151621	0.00950342
0.31 - 0.32	0.00520607	0.00509567	0.81 - 0.82	0.01127841	0.01127841
0.32 - 0.33	0.00584304	0.00566468	0.82 - 0.83	0.01149923	0.01236549
0.33 - 0.34	0.00624219	0.00610631	0.83 - 0.84	0.01188140	0.01250987
0.34 - 0.35	0.00696408	0.00664984	0.84 - 0.85	0.01270521	0.01377530
0.35 - 0.36	0.00761802	0.00731228	0.85 - 0.86	0.01406405	0.01555029
0.36 - 0.37	0.00837389	0.00795773	0.86 - 0.87	0.01501524	0.01591548
0.37 - 0.38	0.00928261	0.00897687	0.87 - 0.88	0.01655243	0.01791128
0.38 - 0.39	0.01020832	0.00967328	0.88 - 0.89	0.01797073	0.02045912
0.39 - 0.40	0.01142279	0.01072638	0.89 - 0.90	0.02146976	0.02348255
0.40 - 0.41	0.01275616	0.01177099	0.90 - 0.91	0.02111306	0.02049309
0.41 - 0.42	0.01457362	0.01338463	0.91 - 0.92	0.01547385	0.01556727
0.42 - 0.43	0.01686667	0.01539741	0.92 - 0.93	0.01329120	0.01325724
0.43 - 0.44	0.01998352	0.01745267	0.93 - 0.94	0.01129540	0.01154169
0.44 - 0.45	0.02552931	0.02175002	0.94 - 0.95	0.00972424	0.00997052
0.45 - 0.46	0.03735127	0.02511317	0.95 - 0.96	0.00850128	0.00858621
0.46 - 0.47	0.03945748	0.03113455	0.96 - 0.97	0.00710846	0.00716791
0.47 - 0.48	0.02909628	0.03848080	0.97 - 0.98	0.00575811	0.00586002
0.48 - 0.49	0.02639557	0.02910477	0.98 - 0.99	0.00425489	0.00433132
0.49 - 0.50	0.02501974	0.02659091	0.99 - 1.00	0.00219113	0.00215717

EXPLANATION OF PLATE VI

Fig. 7. Three calculated frequency histograms for vanadium with $\gamma_2/\gamma_1 = 0.0$ (upper curve), $\gamma_2/\gamma_1 = 0.5$ (middle curve), and $\gamma_2/\gamma_1 = 1.0$ (bottom curve).

NOTE: For display purposes, while the scale of the ordinate is the same for all three curves, the origin for the middle curve is at 0.02 and is at 0.04 for the upper curve.

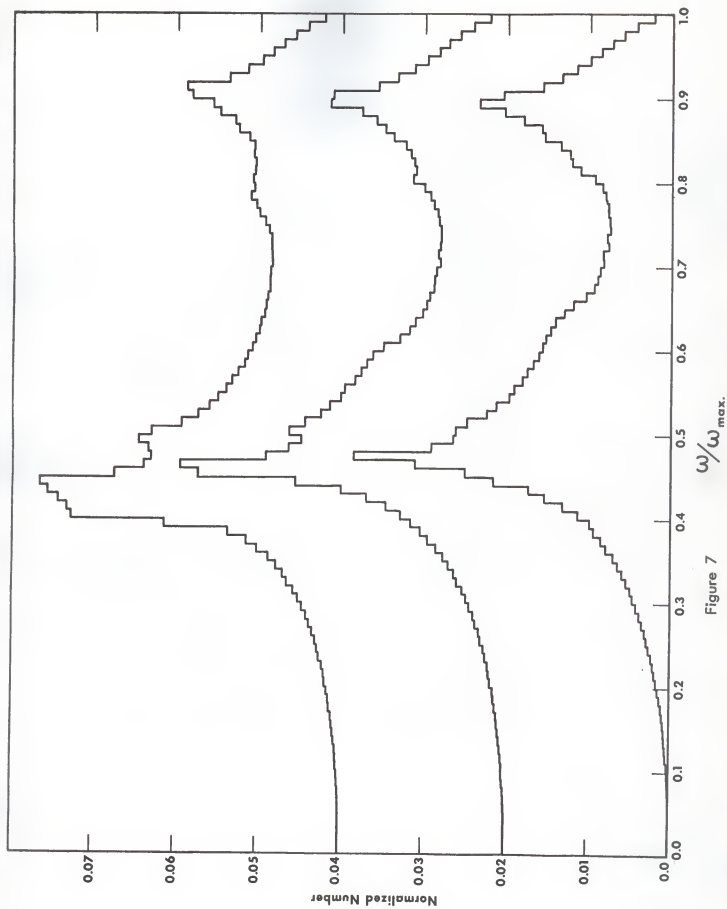


Figure 7

Table 4 (cont.). Frequency distribution histogram using Aiers' elastic constants, and $\pm 10\%$ values of those constants.

Frequency interval	:Aiers constants			:Fraction in interval			:Fraction in interval			:Fraction in interval		
	:C ₁₁ up 10%	:C ₁₁ down 10%	:C ₁₂ up 10%	:C ₁₁ down 10%	:C ₁₂ up 10%	:C ₁₂ down 10%	:C ₄₄ up 10%	:C ₄₄ down 10%	:C ₄₄ up 10%	:C ₄₄ down 10%	:C ₄₄ up 10%	:C ₄₄ down 10%
0.30 - 0.31	0.00522306	0.00502773	0.00550332	0.00607233	0.00450967	0.00483239	0.00586002					
0.31 - 0.32	0.00569866	0.00557975	0.00625069	0.00685669	0.00683688	0.00522306	0.00657341					
0.32 - 0.33	0.00651396	0.00622521	0.00687066	0.00768597	0.00551181	0.00574961	0.00749063					
0.33 - 0.34	0.00711695	0.00693011	0.00773692	0.00879003	0.00608337	0.00637808	0.00823800					
0.34 - 0.35	0.00794924	0.00770295	0.00867113	0.01074337	0.00680272	0.00713394	0.00962232					
0.35 - 0.36	0.00880702	0.00866264	0.00974122	0.01589849	0.00731228	0.00767747	0.01134636					
0.36 - 0.37	0.01021682	0.00977519	0.01142279	0.02260779	0.00817855	0.00878154	0.01745267					
0.37 - 0.38	0.01140581	0.01115952	0.01529551	0.02981816	0.00912125	0.00976670	0.02694760					
0.38 - 0.39	0.01368187	0.01285807	0.02549534	0.03043759	0.01034421	0.01102363	0.03262928					
0.39 - 0.40	0.02150373	0.01534646	0.03058252	0.03043814	0.01153320	0.01252685	0.0367389					
0.40 - 0.41	0.03286707	0.02495180	0.03091373	0.03191588	0.01318080	0.01480292	0.03537245					
0.41 - 0.42	0.03331719	0.03734277	0.03141481	0.03217067	0.01562672	0.02002598	0.03647651					
0.42 - 0.43	0.03444673	0.03913475	0.03202629	0.03422592	0.01880302	0.03413250	0.02894341					
0.43 - 0.44	0.03556778	0.04255734	0.03192437	0.03059950	0.03300296	0.03435332	0.02244643					
0.44 - 0.45	0.03659541	0.02924915	0.03242545	0.02496879	0.04018786	0.03459111	0.02118100					
0.45 - 0.46	0.02751662	0.02256533	0.03239148	0.02374583	0.04245543	0.03588201	0.02026378					
0.46 - 0.47	0.02398362	0.02097718	0.02843384	0.02476496	0.03178000	0.03432783	0.02022981					
0.47 - 0.48	0.02309188	0.02153377	0.02615777	0.02117251	0.02665035	0.02779688	0.01998352					
0.48 - 0.49	0.02340611	0.02017885	0.02231903	0.01888795	0.02407704	0.02637859	0.02057801					
0.49 - 0.50	0.02450168	0.01983166	0.01957373	0.01720638	0.02259929	0.02800071	0.02076486					
0.50 - 0.51	0.02298147	0.02022981	0.01787731	0.01602589	0.02259929	0.02756758	0.02108758					
0.51 - 0.52	0.01947396	0.02031674	0.01669681	0.01488785	0.02315982	0.02328721	0.01837838					
0.52 - 0.53	0.01746117	0.02106211	0.01530400	0.01419144	0.02388171	0.01996654	0.01640806					
0.53 - 0.54	0.01595794	0.02192837	0.01454814	0.01344407	0.02486687	0.01804717	0.01483689					
0.54 - 0.55	0.01503222	0.01858221	0.01348654	0.01258630	0.02039967	0.01624669	0.01388570					
0.55 - 0.56	0.01401309	0.01636560	0.01305341	0.01193236	0.01815757	0.01527002	0.01329970					
0.56 - 0.57	0.01323175	0.01516811	0.01223810	0.01158416	0.01607684	0.01435281	0.01247590					
0.57 - 0.58	0.01257781	0.01395564	0.01167758	0.01090473	0.01490483	0.01334216	0.01181346					
0.58 - 0.59	0.01181346	0.01302793	0.01142253	0.01064995	0.01411501	0.01278163	0.01137184					
0.59 - 0.60	0.01140581	0.01243343	0.01073488	0.01024230	0.01312135	0.01200879	0.01089624					

Table 4 (cont.). Frequency distribution histogram using Alers' elastic constants, and $\pm 10\%$ values of those constants.

Frequency interval	:Fraction in			:Fraction in			:Fraction in		
	:interval	:interval	:interval	:interval	:interval	:interval	:interval	:interval	
:Alers constants	:C ₁₁ up 10%	:C ₁₁ down 10%	:C ₁₂ up 10%	:C ₁₂ down 10%	:C ₄₄ up 10%	:C ₄₄ down 10%	:C ₄₄ up 10%	:C ₄₄ down 10%	
0.60 - 0.61	0.01080282	0.01171155	0.01035270	0.00986012	0.01256083	0.01150772	0.01032722	0.01032722	
0.61 - 0.62	0.01055653	0.01134636	0.00996204	0.00958835	0.01178798	0.01107459	0.01006395	0.01006395	
0.62 - 0.63	0.01008943	0.01065844	0.00973273	0.00935055	0.01129540	0.01058201	0.00967328	0.00967328	
0.63 - 0.64	0.00988560	0.01036119	0.00931658	0.00918069	0.01070940	0.01006395	0.00960533	0.00960533	
0.64 - 0.65	0.00937603	0.01010641	0.00903632	0.00878154	0.01039517	0.00991108	0.00924015	0.00924015	
0.65 - 0.66	0.00924015	0.00969026	0.00883249	0.00855223	0.00989751	0.00950342	0.00891742	0.00891742	
0.66 - 0.67	0.00907029	0.00938453	0.00882400	0.00852675	0.00972424	0.00937603	0.00877904	0.00877904	
0.67 - 0.68	0.00871360	0.00912125	0.00861168	0.00850128	0.00946945	0.00901934	0.00865415	0.00865415	
0.68 - 0.69	0.00871360	0.00895140	0.00862867	0.00835690	0.00919768	0.00892591	0.00853524	0.00853524	
0.69 - 0.70	0.00870510	0.00881550	0.00831443	0.00826348	0.00909577	0.00872209	0.00852675	0.00852675	
0.70 - 0.71	0.00844183	0.00872209	0.00841635	0.00828046	0.00876455	0.00868811	0.00833991	0.00833991	
0.71 - 0.72	0.00846730	0.00872209	0.00841635	0.00843333	0.00881550	0.00857771	0.00838237	0.00838237	
0.72 - 0.73	0.00856922	0.00867113	0.00863716	0.00850128	0.00863716	0.00850128	0.00845031	0.00845031	
0.73 - 0.74	0.00867113	0.00862017	0.00878154	0.00876455	0.00885797	0.00872209	0.00873058	0.00873058	
0.74 - 0.75	0.00892591	0.00885797	0.00914673	0.00912125	0.00879003	0.00896838	0.00888345	0.00888345	
0.75 - 0.76	0.00929960	0.00907879	0.01006395	0.01002149	0.00902782	0.00922316	0.00937603	0.00937603	
0.76 - 0.77	0.01008093	0.00950342	0.01053955	0.01070090	0.00935055	0.00984313	0.01031024	0.01031024	
0.77 - 0.78	0.01059899	0.01022531	0.01008093	0.01007244	0.01002998	0.01098966	0.01056502	0.01056502	
0.78 - 0.79	0.01117650	0.01124445	0.01045462	0.01011490	0.01117650	0.01069241	0.01105760	0.01105760	
0.79 - 0.80	0.01070090	0.01117650	0.01014888	0.01034421	0.01160114	0.01115102	0.01076885	0.01076885	
0.80 - 0.81	0.01093021	0.01188990	0.01016586	0.01016586	0.01014143	0.01082830	0.01044612	0.01044612	
0.81 - 0.82	0.01069241	0.01098116	0.01012339	0.01023380	0.01128853	0.01070940	0.01087076	0.01087076	
0.82 - 0.83	0.01047160	0.01141430	0.01010641	0.00979218	0.01244445	0.01078583	0.01053105	0.01053105	
0.83 - 0.84	0.01081131	0.01109158	0.01020832	0.01031873	0.01112554	0.01063296	0.01038668	0.01038668	
0.84 - 0.85	0.01078583	0.01110007	0.01083679	0.01057351	0.01126992	0.01103213	0.01075187	0.01075187	
0.85 - 0.86	0.01143128	0.01150772	0.01155867	0.01117650	0.01174552	0.01182196	0.01130389	0.01130389	
0.86 - 0.87	0.01262877	0.01242494	0.01241645	0.01228056	0.01301094	0.01268822	0.01217016	0.01217016	
0.87 - 0.88	0.01309587	0.01335914	0.01349504	0.01323724	0.01345257	0.01374982	0.01314683	0.01314683	
0.88 - 0.89	0.01490483	0.01439527	0.01487087	0.01399611	0.01485388	0.01483689	0.01405556	0.01405556	
0.89 - 0.90	0.01567768	0.01564371	0.01605985	0.01588151	0.01633162	0.01660340	0.01537194	0.01537194	

Table 4 (concl.). Frequency distribution histogram using Alers' elastic constants, and $\pm 10\%$ values of those constants.

Frequency interval	:Fraction in :interval			:Fraction in :interval			:Fraction in :interval			:Fraction in :interval		
	:Alers constants	:C ₁₁ up 10%	:C ₁₁ down 10%	:C ₁₁ up 10%	:C ₁₁ down 10%	:C ₁₂ up 10%	:C ₁₂ down 10%	:C ₄₄ up 10%	:C ₄₄ down 10%	:C ₄₄ up 10%	:C ₄₄ down 10%	
0.90 - 0.91	0.01823401	0.01786032	0.01890494	0.01803018	0.01852276	0.01878604	0.01756307					
0.91 - 0.92	0.01890494	0.01955888	0.01785183	0.01783484	0.01982216	0.01923615	0.01855673					
0.92 - 0.93	0.01377530	0.01427637	0.01338463	0.01341860	0.01453115	0.01396213	0.01371585					
0.93 - 0.94	0.01158416	0.01189839	0.01124445	0.01101514	0.01213618	0.01177099	0.01131239					
0.94 - 0.95	0.00983464	0.01006395	0.00971574	0.00961383	0.01019983	0.00997902	0.00981766					
0.95 - 0.96	0.00848429	0.00867113	0.00824649	0.00808513	0.00885797	0.00869661	0.00834841					
0.96 - 0.97	0.00717640	0.00729530	0.00694709	0.00693860	0.00743119	0.00721887	0.00693860					
0.97 - 0.98	0.00572413	0.00591947	0.00569866	0.00561373	0.00597892	0.00581755	0.00579207					
0.98 - 0.99	0.00428885	0.00434830	0.00419543	0.00410201	0.00442474	0.00436529	0.00416996					
0.99 - 1.00	0.00219113	0.00219963	0.00214867	0.00210620	0.00225058	0.00220812	0.00213169					

Table 5. Maximum frequency in cycles per second for vanadium elastic constants varied by $\pm 10\%$.

$C_{11} \times 10^{-12}$ dyne -cm ⁻²	$C_{12} \times 10^{-12}$ dyne -cm ⁻²	$C_{44} \times 10^{-12}$ dyne -cm ⁻²	Maximum frequency in c.p.s.	Elastic constant varied
2.2795	1.1870	0.4255	8.866×10^{12}	Alers constants
2.5074	1.1870	0.4255	9.097×10^{12}	C_{11} up 10%
2.0516	1.1870	0.4255	8.628×10^{12}	C_{11} down 10%
2.2795	1.3057	0.4255	8.987×10^{12}	C_{12} up 10%
2.2795	1.0683	0.4255	8.743×10^{12}	C_{12} down 10%
2.2795	1.1870	0.4605	8.953×10^{12}	C_{44} up 10%
2.2795	1.1870	0.3830	8.778×10^{12}	C_{44} down 10%

dispersion curves for iron as determined by Low (21). Using the elastic constants given by Low (21) for iron at 16°C as

$$\begin{aligned} C_{11} &= 2.332 \times 10^{12} \text{ dyne-cm}^{-2} \\ C_{12} &= 1.355 \times 10^{12} \text{ dyne-cm}^{-2} \\ C_{44} &= 1.180 \times 10^{12} \text{ dyne-cm}^{-2} , \end{aligned}$$

dispersion curves were calculated along the (101), (111), and (001) directions. The results of these calculations are shown in Figs. 8, 9, and 10. For comparison the same calculations were performed using a two constant central force model. These calculations showed that the shape of the dispersion curves remained essentially the same; however, the maximum frequency of 9.735×10^{12} cps for the three constant model was higher than the maximum frequency of 8.711×10^{12} cps found for the two constant model. Comparison with Low's curves showed that the three constant model represented experiment better than did the two constant model; however, both were quite good. For example at the point of three fold degeneracy along the (001) direction Low has about .034 ev, the three constant model gives .0354 ev, and the two constant model gives .0325 ev. For the higher of the two transverse modes along the (101) direction at the zone boundary the three constant model gives .0252 ev, the two constant model .0232 ev, and Low has approximately .027 ev. At the point of three fold degeneracy along the (111) direction the model employed here gives .0308 ev, the central force model gives .0276 ev, and Low has approximately .030 ev. For the maximum value of the longitudinal wave along the (111) direction Low has approximately .037 ev, while the three constant model gives .0363 ev, and the two constant model .0325 ev. In general, the inclusion of the angular stiffness terms have improved the agreement with experiment in this case.

EXPLANATION OF PLATE VII

Fig. 8. Dispersion curves for iron along the (101) direction,
 $\epsilon_1 = \epsilon_3 = \epsilon$, $\epsilon_2 = 0$ where $\epsilon = \text{max}_1$.

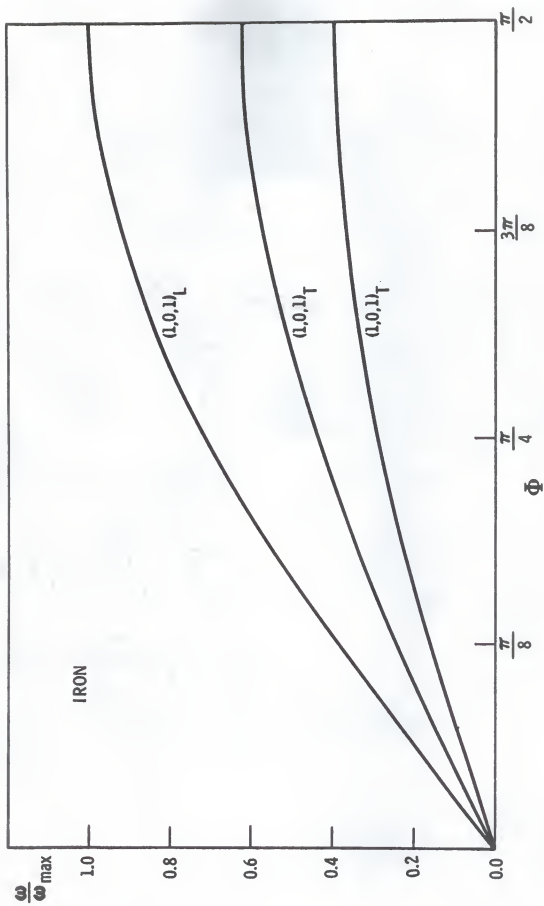


Figure 8

EXPLANATION OF PLATE VIII

Fig. 9. Dispersion curves for iron along the (111) direction,
 $\xi_1 = \xi_2 = \xi_3 = \xi$, where $\xi_1 = \pi a k_1$.

PLATE VIII

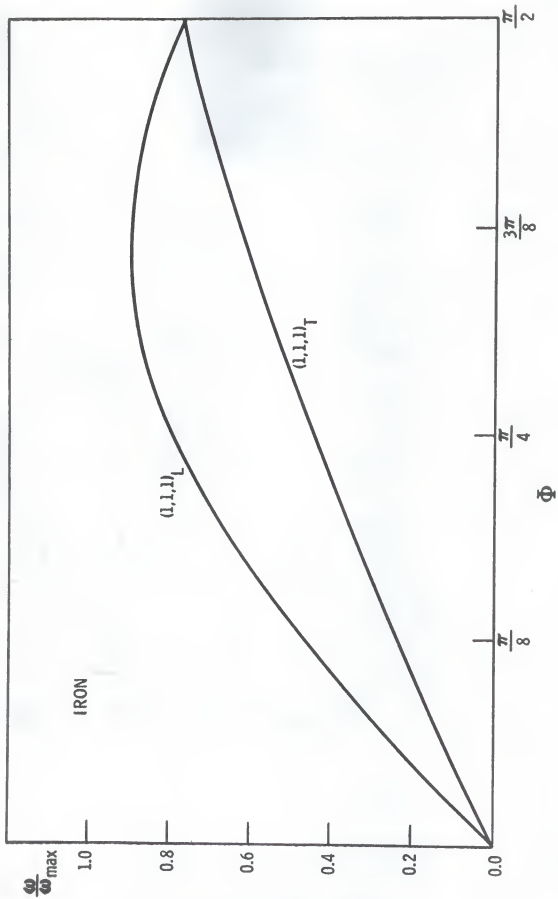


Figure 9

EXPLANATION OF PLATE IX

Fig. 10. Dispersion curves for iron along the (001) direction,
 $\psi_1 = \psi_2 = 0$, where $\psi_3 = \pi a k_3$.

PLATE IX

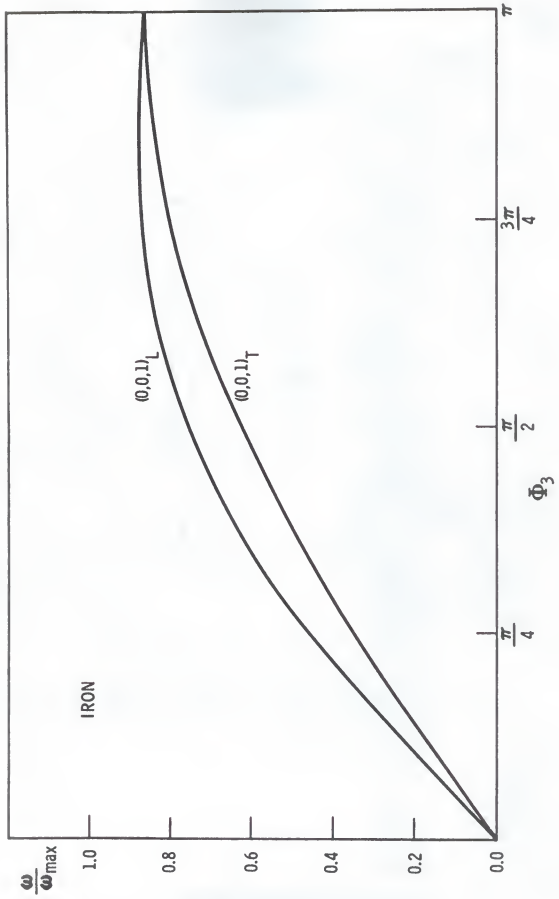


Figure 10

CONCLUSION

The dynamical properties of a body centered cubic lattice of identical particles have been investigated using the Born-von-Karman model of a crystal lattice. The model employed contained non-central as well as central forces, thus the Cauchy relation is not required. In particular, the forces between lattice points consisted of non-central angular stiffness forces and central forces between nearest and next-nearest neighbors. The non-central angular stiffness force constants γ_1 and γ_2 and the central force constants α and β were identified with the elastic constants of the material by the usual comparison with continuum theory.

Frequency distribution histograms have been constructed for vanadium and compared with the experimental frequency distributions available from slow neutron experiments. Qualitative agreement was found in so far as the shapes of the experimental and theoretical distributions were concerned, in that both distributions showed two pronounced peaks. The calculated maximum frequency for vanadium was in good agreement with that derived from the experimental frequency distributions, which constitutes an improvement over the results of the central force model. It has also been shown that the addition of the fourth force constant, γ_2 , could be used to alter the shape of the frequency distribution without destroying the agreement between theoretical and experimental maximum frequency. Vanadium distributions were also calculated with each elastic constant varied independently by ± 10 per cent. These distributions also exhibited qualitative agreement with experiment, and the calculated maximum frequencies were generally in good agreement with experiment. For tungsten, since no direct experimental results are available

the calculated distribution was compared with previous theoretical results. This calculation was performed with $\gamma_2 = 0$ and the resulting distribution contained two peaks as does the distribution from the two constant central force model; however, the maximum frequency calculated with central forces only was approximately 25 per cent lower than that from the model used here. Dispersion curves for iron were also calculated and found to be in good qualitative and quantitative agreement with experiment.

The calculations performed using this model indicate that it exhibits a more reasonable behavior than the models generally used for cubic crystals. It would appear that the improvement is due in part to the removal of the restrictive and unrealistic Cauchy relation. In view of these results it would be of interest to adapt this model to face centered cubic crystals.

ACKNOWLEDGMENTS

The author deeply appreciates the encouragement and council of her major advisors Dr. Basil Curnutte, Associate Professor, Department of Physics, Kansas State University, and Dr. Robert Herman, Head, Department of Theoretical Physics, General Motors Research Laboratories. The author also acknowledges the valuable advice and many helpful discussions of Dr. David Evans, General Motors Research Laboratories, Dr. Denos C. Gazis, Thomas Watson Research Center, and Dr. Richard F. Wallis, U.S. Naval Research Laboratory. In addition the author thanks Dr. Thomas J. Clark for reading the manuscript and for continued moral support.

REFERENCES

1. Debye, Peter
Collected papers. New York: Interscience, 1954. 650 p.
2. Born, Max, and T. Von-Karman
Über schwingungen in ramgittern.
Physik Zeits. 13, 1912. 297 p.
3. Blackman, M.
Contributions to the theory of the specific heat of crystals I and II.
Proc. Roy. Soc. London. A 148, 1935, 365 p and 385 p.
4. Blackman, M.
On the vibrational spectrum of a three dimensional lattice.
Proc. Roy. Soc. London. A 156, 1937. 416 p.
5. Montroll, E.W.
Dynamics of a square lattice.
J. Chem. Phys. 15:8, 1947. 575 p.
6. Bowers, W.A., and H.B. Rosenstock
On the vibrational spectra of crystals.
J. Chem. Phys. 18:8, 1950. 1056 p.
7. Van Hove, Leon
The occurrence of singularities in the elastic frequency distribution
of a crystal.
Phys. Rev. 89:6, 1953. 1189 p.
8. Phillips, J.C.
Critical points and lattice vibration spectra.
Phys. Rev. 104:5, 1956. 1263 p.
9. Fine, C.P.
The normal modes of vibration of a body-centered cubic lattice.
Phys. Rev. 56, 1939. 355 p.
10. Clark, C.B.
Calculated frequency spectra for body-centered cubic lattices.
Journal of the Graduate Research Center, 26:1, 1961. 10 p.
11. Leighton, R.B.
The vibrational spectrum and specific heat of a face-centered cubic
crystal.
Rev. Mod. Phys., 20:1, 1948. 165 p.
12. Shankland, D.C.
Vibrational distribution functions for cubic lattices.
Bul. Am. Phys. Soc., Series II, 7, 1962. 17 p.

13. Montroll, E.W. and D.C. Peasly
Frequency spectrum of crystalline solids.
J. Chem. Phys. 10, 1942. 218 p.
14. Montroll, E.W.
Frequency spectrum of crystalline solids.
J. Chem. Phys. 10, 1942. 218 p.
15. Smith, H.M.J.
The theory of the vibrations and the Raman spectrum of the diamond lattice.
Trans. Roy. Soc. London. A 241, 105, 1948. 105 p.
16. Rosenstock, H.B. and G.F. Newell
Vibrations of a simple cubic lattice. I.
J. Chem. Phys. 21, 1953. 1607 p.
17. Singh, D.N., and W.A. Bowers
Vibrational spectrum of vanadium.
Phys. Rev. 116:2, 1959. 279 p.
18. Gazis, D.C., Robert Herman, and R.F. Wallis
Surface elastic waves in cubic crystals.
Phys. Rev. 119:2, 1960. 533 p.
19. Stewart, A.T., and B.N. Brockhouse
Vibration spectra of vanadium and a Mn-Ce alloy by neutron spectrometry.
Rev. Mod. Phys. 30:1, 1958. 250 p.
20. Eisenhauer, C.M., et. al.
Measurement of lattice vibrations in vanadium by neutron scattering.
Phys. Rev. 109:4, 1958. 1046 p.
21. Low, G.G.E.
Some measurements of phonon dispersion relations in iron.
Proc. Phys. Soc. London. 79, 1962. 479 p.
22. DeLaunay, Jules
Solid state physics, Vol. 2. New York: Academic Press, 1956.
23. Born, Max, and Kun Huang
Dynamical theory of crystal lattices. Oxford: Clarendon Press, 1954.
24. Brillouin, Leon
Wave propagation in periodic structures. Dover Publications, 1953.
25. Quimby, S.L., and Sidney Siegel
The variation of the elastic constants of crystalline sodium with temperature between 80°K and 210°K.
Phys. Rev. 54, 1938. 293 p.

26. Joos, Georg
Theoretical physics. 3rd ed. New York. Hafner, Chapt. VIII.
27. Zener, Clarence
Elasticity and anelasticity of metals. Chicago: University of Chicago Press. 1948. 15 p.
28. Alers, G.A.
Elastic moduli of vanadium.
Phys. Rev. 119:5, 1960. 1532 p.
29. Barnard, S., and J.M. Child
Higher algebra. London: Macmillan. 1939. 180 p.

FREQUENCY SPECTRUM OF ELASTIC WAVES
IN BODY CENTERED CUBIC LATTICES

by

BUNNY COWAN CLARK

B.S., Kansas State University, 1958

AN ABSTRACT OF A THESIS

submitted in partial fulfillment of the

requirements for the degree

MASTER OF SCIENCE

Department of Physics

KANSAS STATE UNIVERSITY

1963

ABSTRACT

The Born-von Karman model of a crystal lattice has been used to investigate the dynamical properties of a body centered cubic lattice of identical particles. A two-constant model using central force interactions between nearest and next-nearest neighbors has most frequently been employed by other investigators. The use of central forces has the disadvantage of requiring that the Cauchy relation be satisfied between elastic constants of the crystal. The model used in this work contains non-central as well as central forces. As a consequence it has the inherent advantage of removing the requirement of the Cauchy relation. In particular, the forces between lattice points consist of non-central angular stiffness forces as well as central forces between nearest and next-nearest neighbors. The force constants employed can be identified from continuum theory in the usual way with the elastic constants of the lattice.

Plane wave solutions to the equations of motion result in a secular equation for the characteristic frequencies of the lattice. The roots of this equation were found numerically at approximately 39,000 points using an IBM 7090 digital computer. Frequency distribution histograms have been constructed for vanadium and compared with the experimental frequency distributions available from slow neutron experiments. Qualitative agreement was found in so far as the shapes of the experimental and theoretical distributions were concerned. The calculated maximum frequency for vanadium was in good agreement with that derived from the experimental frequency distributions. This constitutes an improvement over the results of the simpler central force model. Histograms were calculated for tungsten and compared with previous theoretical results since no direct experimental results for tungsten are available. Dispersion curves for iron were also calculated and found to be in good agreement

with experiment.

The present model has the advantage that the Cauchy relation is not required. In addition, the calculations performed using this model indicate that it exhibits a more reasonable behavior than the model generally used heretofore for cubic crystals.